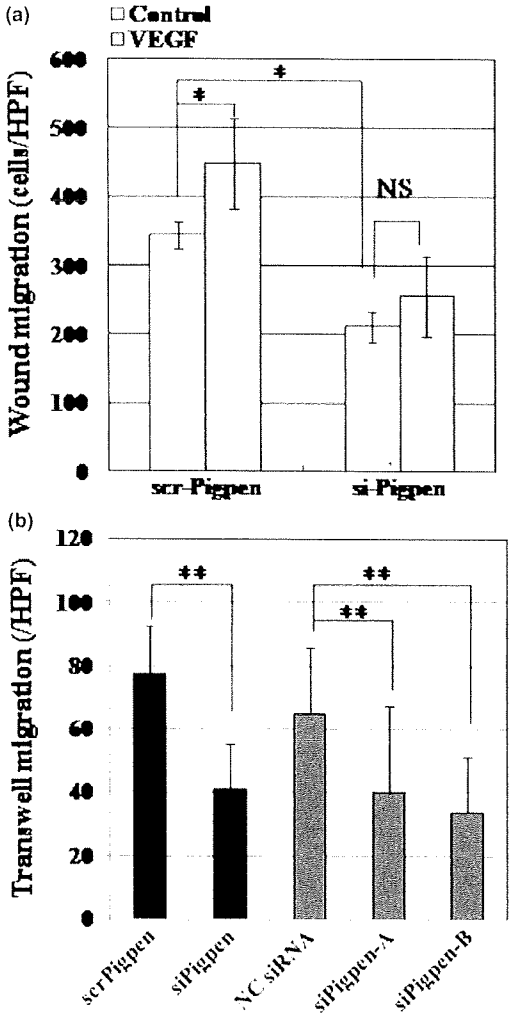


Fig. 4. (a) Wound migration assay of scr- or siPigpen-transfected MS1 cells with vehicle or 50 ng/mL vascular endothelial growth factor (VEGF) ($n = 6$). (b) Transwell migration assay of MSS31 cells transfected with scr- or siPigpen, nontargeting control siRNA (NC siRNA), siPigpen-A, or siPigpen-B ($n = 12$). Data indicate means and SDs. $^*P < 0.05$, $^{**}P < 0.01$.

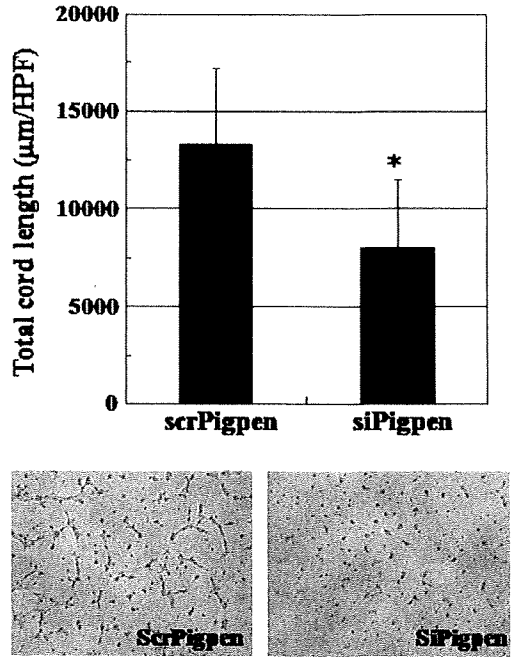


Fig. 5. Network formation of MS1 cells transfected with scr- or siPigpen. Data indicate means and SDs, $n = 6$. $^*P < 0.05$. Repre sentative images are shown.

HG-DMEM with or without 20 ng/mL bFGF and MS1 cells were incubated for an additional 24 h. MSS31 cells were incubated for 48 h. Cell numbers were analyzed with a Cell Titer 96 Aqueous Assay (Promega, Madison, WI, USA).

**EC wound migration assay.** At 10 h after transfection of scr- or siPigpen into MS1 cells, medium was changed to growth medium. After 14-h incubation, cells were replated into 12-well plates at a density of 200 000/well. The next day, confluent monolayers were wounded with a yellow tip, and cells were incubated in 0.1% HG-DMEM for an additional 24 h. Cells that had migrated into the denuded area were counted.

**Transwell migration assay.** MSS31 cells were transfected with scr- or siPigpen, NC siPigpen, siPigpen-A, or siPigpen-B. Next day cells were starved in 0.1% αMEM for 2 h and replated in 0.1% αMEM on a filter of 8-μm pore size in the upper insert of 24-well transwell chambers (Corning, Acton, MA, USA) at the density of 47 500 cells/95 μL/well. Six-hundred microliter of 0.1% αMEM with or without 20 ng/mL bFGF was added into the lower chamber. After 7-h incubation, unmigrated cells on the upper side of the filter were scraped off with a cotton swab and the filters were fixed and stained with 0.1% crystal violet in 70% ethanol for 30 min. Migration was quantified by counting cells in randomly selected high power fields (HPF).

**EC network formation assay.** MS1 cells treated as described above were inoculated onto 96-well plates coated with growth factor-reduced Matrigel (GFR-Matrigel; BD Biosciences) at a density of 20 000 per well. Under these conditions, cells began to form tubes, and 4 h later, the tube length was measured with a BZ Analyzer (Keyence, Osaka, Japan).

**Matrigel plug assay.** GFR-Matrigel (500 μL) containing 100 ng/mL bFGF (BD Biosciences), 32 U/mL heparin, and 200 nM scr- or siPigpen was subcutaneously injected into 5-week-old male C57BL/6 mice. On day 6, Matrigel was removed for immunohistochemistry (IHC) of vascular endothelial (VE)-cadherin and hemoglobin (Hb) measurement. Hb content was measured using a hemoglobin B test (Wako, Osaka, Japan). The number of blood vessels positive for VE-cadherin was counted under a fluorescent microscope (Biozero BZ-8000, Keyence).

**Syngenic tumor implantation model.** A mixture of 150 μL GFR-Matrigel and 150 μL of Hanks' Balanced Salt Solution (HBSS) containing 500 000 LLC cells was subcutaneously injected into 5-week-old male C57BL/6 mice. On day 5, 100 pmol scr- or siPigpen was injected into the tumors. Every 3 days, the tumor volume was measured with calipers, and the injection of scr- or siPigpen was repeated. Tumor volume was estimated by using the formula of $a$ (the major axis) $\times$ $b$ (the minor axis)$^2/2$. On day 14, tumors were removed for IHC for CD31, and the length of CD31-positive tubes was measured with a BZ Analyzer (Keyence).

All protocols for experiments involving animals were approved by the Tokyo Medical and Dental University Bioethical and Animal Care Ethics Committees and conformed to the provisions of the Declaration of Helsinki in 1995 (as revised in Tokyo in 2004).

**IHC analysis.** Tissues from the Matrigel plug assay and the syngenic tumor implantation model were harvested, embedded



doi: 10.1111/j.1349-7006.2010.01494.x
© 2010 Japanese Cancer Association

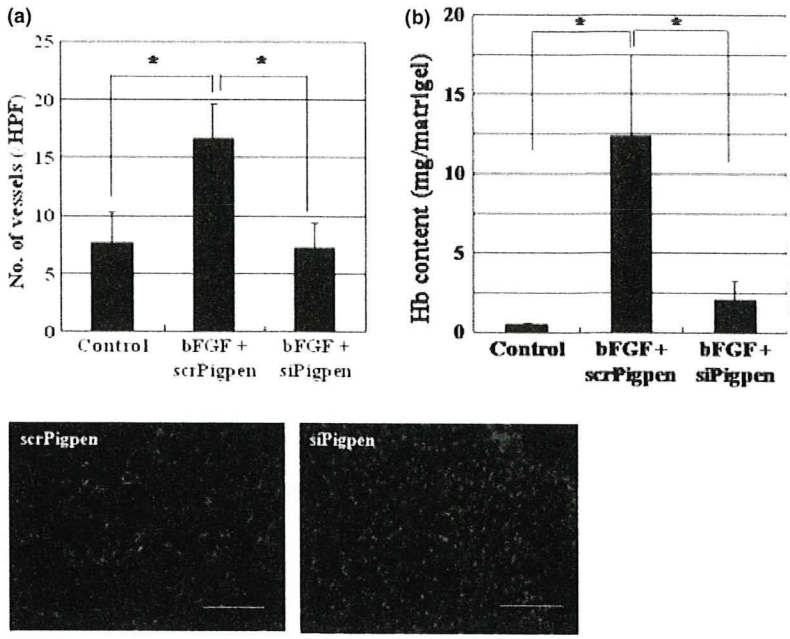


Fig. 6. Matrigel plug assay was performed as described in the Materials and Methods. On day 6, blood vessels positive for vascular endothelial (VE)-cadherin were counted (a) and hemoglobin content in the Matrigels was measured (b). Data indicate means and SEs (a) or SDs (b). $n = 12$ (Control) or 15 (basic fibroblast growth factor [bFGF] + scr- or siPigpen) in (a); $n = 5$ (Control and bFGF + siPigpen) or 6 (bFGF + siPigpen) in (b). $^*P < 0.05$. Representative immunohistochemistry (IHC) of VE-cadherin (red) and nuclei (blue) is shown. Scale bar = 100 μm. Hb, hemoglobin.

in OCT compound (Sakura Finetechnical, Tokyo, Japan), and snap-frozen in liquid nitrogen. Thin sections (5–6 μm) were cut on a cryostat (Leica CM1850, Leica MZFLIII; Leica Microsystems, Wetzlar, Germany) and collected on glass slides. Specimens were dried for 30 min and fixed in 4% PFA in 0.1 M PBS for 10 min. After washing with PBS, specimens were incubated in BS for 1 h, and then incubated with 2 μg/mL anti-VE-cadherin (Alexis Biochemicals, San Diego, CA, USA) or 1/100 (v/v) antimouse CD31 monoclonal (Fitzgerald Industries International, Concord, MA, USA) and 10 μg/mL antimouse pigpen rat IgG in RB for 1 h. After three washes with PBS, specimens were incubated with 4 μg/mL Alexa Fluor 546 goat antirabbit and rat IgG (Invitrogen) for VE-cadherin and CD31, respectively, or Alexa Fluor 488 goat antirabbit IgG (Invitrogen) for pigpen in RB for 1 h, washed with PBS three times, and incubated with Hoechst 33342 or TO-PRO-3 for nuclear staining. After a tap water rinse, VE-cadherin, CD31, and pigpen signals in endothelial cells were observed under a fluorescent microscope (Biozero BZ-8000, Keyence).

**Statistical analysis.** The statistical significance of differences was evaluated by ANOVA, and $P$-values were calculated using the Student's $t$-test. A value of $P < 0.05$ was considered statistically significant. The statistical calculation was done using JMP software (SAS, Cary, NC, USA).

## Results

**PILSAP activity regulated the expression of pigpen, a coiled body component protein.** We previously showed that among vascular endothelial growth factor receptor 2 (VEGFR2)-positive precursor cells, including vascular, hematopoietic, and muscle lineages, only ECs continued to express VEGFR2 until terminal differentiation in an *in vitro* mouse ES differentiation culture system.[9] The time course of VEGFR2 expression in EBs showed two peaks at days 4 and 10, indicating expansion of VEGFR2-positive mesodermal precursors and endothelial lineages, respectively.[9] To clarify the mechanisms of how PILSAP plays a role in differentiation or maturation of ECs, we searched for molecules whose expression was correlated with the AP activity of PILSAP. On day 8, after day 7 when the expression of PILSAP was lowest and before day 10, the second peak when other EC markers including CD31 and Tie-2 peaked as well,[9] nuclear protein was extracted from mtPILSAP and mock EBs, and proteome analysis was performed. Pigpen was identified as a molecule whose expression was reduced to less than half in mtPILSAP EBs compared with mock EBs.

**Binding of pigpen to PILSAP.** The previous result that the AP activity of PILSAP regulates pigpen expression during EC differentiation does not necessarily indicate that pigpen directly interacts with PILSAP in ECs. Therefore, we examined whether pigpen could bind to PILSAP. Immunoprecipitation with anti-PILSAP followed by western blotting of pigpen and PILSAP demonstrated binding between these two molecules in a mouse endothelial cell line, MSS31. Furthermore, the binding was induced by a 20-min treatment with the representative angiogenic growth factors, VEGF and bFGF in ECs (Fig. 1a,b). Immunocytochemical analysis revealed that pigpen was localized in nuclei, whereas PILSAP was in cytosol and on nuclear membrane. VEGF and bFGF induced translocation of PILSAP from cytosol to nuclei (Fig. 1c). These results suggest that pigpen may be involved in angiogenesis in cooperation with PILSAP upon VEGF and bFGF stimuli.

**SiRNA for pigpen inhibited *in vitro* angiogenesis.** We next investigated whether pigpen plays a role in angiogenesis. We synthesized siRNAs for pigpen and their controls (siPigpen and scrPigpen; NC siRNA, siPigpen-A, and siPigpen-B). SiPigpen strongly inhibited the expression of pigpen protein in mouse endothelial cell lines, MSS31 and MS1 (Fig. 2a) as well as pigpen mRNA (data not shown). The protein level of PILSAP was not altered by transfection of siRNAs for pigpen. Transfection of siPigpen into MSS31 or MS1 abrogated the increase in proliferation by VEGF or bFGF, respectively (Fig. 3a). The decrease in EC proliferation by inhibiting pigpen expression was confirmed by two other siRNAs, namely siPigpen-A and siPigpen-B (Fig. 3b). Moreover, siPigpen significantly inhibited MS1 migration and abrogated the increase by VEGF (Fig. 4a). Inhibition of EC migration by the transfection with three different siRNAs was observed in MSS31 (Fig. 4b). Furthermore, siPigpen significantly inhibited network formation on Matrigel (Fig. 5). These data demonstrate the positive effect of pigpen on EC proliferation, migration, and network formation.


© 2010 Japanese Cancer Association

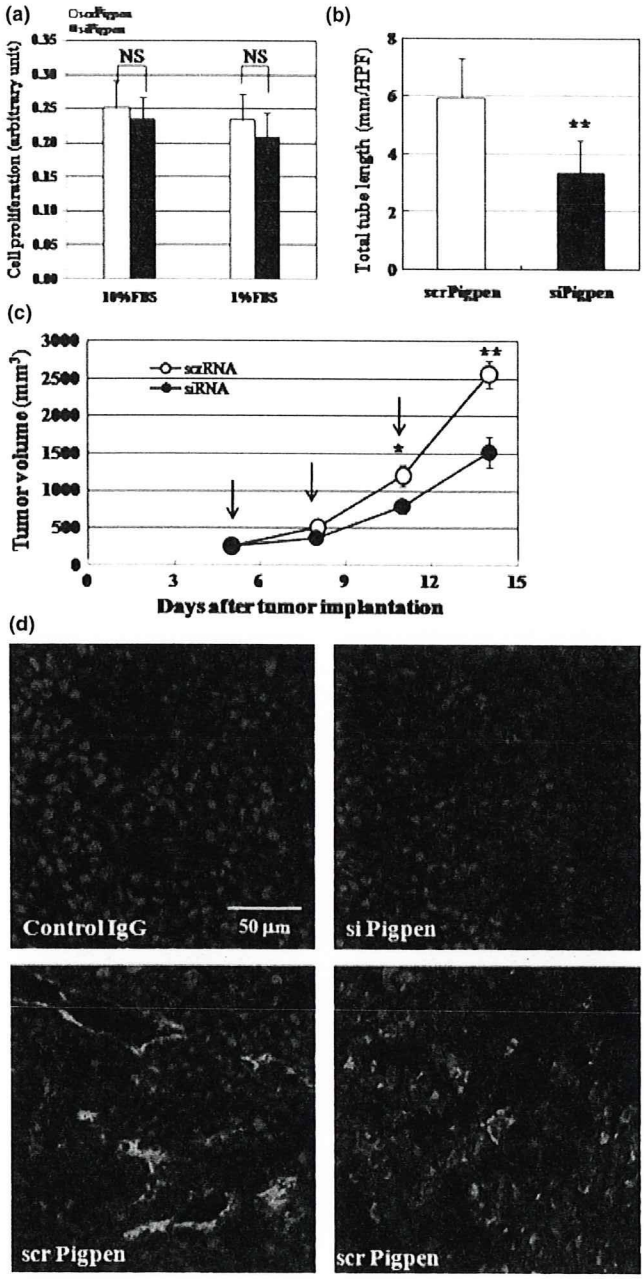


Fig. 7. Syngenic tumor implantation model was performed as described in the Materials and Methods. (a) siPigpen did not inhibit Lewis lung carcinoma (LLC) cell proliferation *in vitro*. Data indicate means and SDs, $n = 10$. (b) siPigpen inhibited tumor growth of LLC. Data indicate means and SEMs, $n = 10$ and 11 for scr- and siPigpen, respectively (days 5, 8, 10) and $n = 8$ (day 14). (c) siPigpen inhibited tumor angiogenesis. Data indicate means and SDs, $n = 15$ (scrPigpen) or 10 (siPigpen). $^{*}P < 0.05$, $^{**}P < 0.01$. (d) Representative immunohistochemistry (IHC) of CD31 (red), pigpen (green), and nuclei (blue) is shown. Bar = 50 μm.

**SiRNA for pigpen inhibited *in vivo* angiogenesis.** Next, we performed a Matrigel plug assay to examine the effect of siPigpen on *in vivo* angiogenesis. GFR-Matrigel containing 100 ng/mL bFGF, heparin, and 200 nM scr- or siPigpen was subcutaneously injected into 5-week-old mice. On day 6, Matrigel was removed, and we measured the Hb content and counted the number of blood vessels that were positive for VE-cadherin in transplanted GFR-Matrigel to analyze blood vessel formation and blood supply. Both the Hb content and blood vessel number were significantly increased by bFGF, and siPigpen abrogated this increase by bFGF (Fig. 6). Thus, pigpen appears to be involved in both *in vitro* and *in vivo* angiogenesis.

**SiRNA for pigpen inhibited tumor growth as well as tumor angiogenesis.** The result showing an inhibitory effect of siPigpen on *in vivo* angiogenesis prompted us to examine whether siPigpen could reduce tumor growth by inhibiting tumor angiogenesis. We employed a syngenic tumor implantation model of LLC. LLC cells express less pigpen than mouse ECs *in vitro* (Fig. 2a, scrPigpen) as well as *in vivo* (Fig. 7d, scrPigpen). Transfection of siPigpen into LLC cells did not alter the proliferation (Fig. 7a). LLC cells in GFR-Matrigel were subcutaneously injected into C57BL/6 mice. On day 5 when tumors became palpable, scr- or siPigpen was injected into the tumor, and the injection was repeated every three days. Figure 7(b) shows the time course of tumor growth in both groups. Injection of siPigpen significantly reduced the tumor size compared with the scrPigpen group on days 10 and 14, after two and three injections, respectively. Immunohistochemical analysis of tumor on day 14 showed the efficient inhibition of pigpen expression by siPigpen (Fig. 7d). The total tube length of blood vessels that were positive for CD31 on day 14 was significantly reduced by siPigpen injection (Fig. 7c,d). These data indicate that pigpen may be a future target for blocking tumor angiogenesis.

## Discussion

We previously isolated PILSAP as a novel angiogenesis factor and showed that the expression of PILSAP is enhanced in mouse cells differentiating from ES cells to ECs.[5] We also demonstrated that PILSAP is involved in postnatal angiogenesis.[5–8] In this study, we searched for a molecule that is related to PILSAP and involved in endothelial differentiation, similar to PILSAP. Proteome analysis using mtPILSAP and mock EBs on day 8 of *in vitro* differentiation cultures revealed that the expression of pigpen, a nuclear coiled body component, was reduced to less than half in mtPILSAP EBs lacking the AP activity. This result suggests that AP activity of PILSAP may regulate pigpen expression, but does not indicate that pigpen directly interacts with PILSAP. However, we detected the complex of PILSAP and pigpen in the nuclear and membrane fractions of EBs and found that the binding was down-regulated in mtPILSAP-EBs (M. Abe, unpublished data, 2008). Pigpen has been suggested to be involved in angiogenesis, especially by inducing EC proliferation and differentiation.[10,11,14,15,16] Therefore, we speculated that pigpen might play a role in angiogenesis in cooperation with PILSAP. First, we examined whether pigpen could bind to PILSAP using IP-Western blotting of mouse EC protein extracts. Although it is known that PILSAP is a cytosolic enzyme[5] and pigpen is a nuclear protein,[11] western blotting using fractionated cell lysates of mouse EBs and ECs revealed that PILSAP localizes predominantly in the cytosol and membrane fractions, whereas pigpen localizes in the nuclear and membrane fractions (M. Abe, unpublished data, 2008). Moreover, ICC of PILSAP and pigpen in MSS31 showed their localization, namely cytosol/nuclear membrane and nucleus/nuclear membrane, respectively (Fig. 1c). The binding of these two molecules were augmented by VEGF and bFGF (Fig. 1a,b). ICC of these molecules demonstrated that VEGF and bFGF induced PILSAP translocation from cytosol to the nucleus/nuclear membrane where pigpen


doi: 10.1111/j.1349-7006.2010.01494.x
© 2010 Japanese Cancer Association

existed (Fig. 1c), although bFGF showed less effect compared with VEGF in these experiments with 20-min incubation (Fig. 1).

Next, we investigated whether pigpen plays a role in postnatal angiogenesis as PILSAP. Three different siRNAs for pigpen inhibited proliferation and migration of MSS31 (Figs 3b and 4b). Although PILSAP regulated pigpen expression, pigpen did not alter PILSAP expression (Fig. 2b). Transfection of siPigpen, one of these siRNAs, inhibited proliferation and migration of two different cell types, MSS31 and MS1, and abrogated the increase in proliferation and migration by VEGF and bFGF (Figs 3–4). Inhibition of pigpen expression resulted in suppression of angiogenesis both *in vitro* (Figs 3–5) and *in vivo* (Fig. 6). Furthermore, injection of siPigpen in syngenic tumors subcutaneously implanted into C57BL/6 mice inhibited tumor growth and tumor angiogenesis (Fig. 7). These findings suggest that the inhibition of pigpen may be useful for therapy of malignant tumors by inhibiting tumor angiogenesis.

We speculate that PILSAP–pigpen complex induced by VEGF and bFGF may play a role in angiogenesis. Further study is needed to clarify whether and how pigpen interacts with PILSAP to promote angiogenesis *in vivo* and whether pigpen is a substrate for PILSAP.

## Acknowledgments

This work was supported in part by a Grant-in-Aid for Scientific Research (no. 17590235) from the Ministry of Education, Science, Sports and Culture of Japan.

## Disclosure Statement

The authors have no conflict of interest.

## References

1 Folkman J. Tumor angiogenesis: therapeutic implications. *N Engl J Med* 1971; **285**: 1182–6.
2 Bergers G, Benjamin LE. Tumorigenesis and the angiogenic switch. *Nat Rev Cancer* 2003; **3**: 401–10.
3 Carmeliet P, Ferreira V, Breier G *et al.* Abnormal blood vessel development and lethality in embryos lacking a single VEGF allele. *Nature* 1996; **380**: 435–9.
4 Ferrara N, Carver-Moore K, Chen H *et al.* Heterozygous embryonic lethality induced by targeted inactivation of the VEGF gene. *Nature* 1996; **380**: 439–42.
5 Miyashita H, Yamazaki T, Akada T *et al.* A mouse orthologue of puromycin-insensitive leucyl-specific aminopeptidase is expressed in endothelial cells and plays an important role in angiogenesis. *Blood* 2002; **99**: 3241–9.
6 Yamazaki T, Akada T, Niizeki O, Suzuki T, Miyashita H, Sato Y. Puromycin-insensitive leucyl-specific aminopeptidase (PILSAP) binds and catalyzes PDK1, allowing VEGF-stimulated activation of S6K for endothelial cell proliferation and angiogenesis. *Blood* 2004; **104**: 2345–52.
7 Akada T, Yamazaki T, Miyashita H *et al.* Puromycin insensitive leucyl-specific aminopeptidase (PILSAP) is involved in the activation of endothelial integrins. *J Cell Physiol* 2002; **193**: 253–62.
8 Suzuki T, Abe M, Miyashita H, Kobayashi T, Sato Y. Puromycin insensitive leucyl-specific aminopeptidase (PILSAP) affects RhoA activation in endothelial cells. *J Cell Physiol* 2007; **211**: 708–15.
9 Abe M, Sato Y. Puromycin insensitive leucyl-specific aminopeptidase (PILSAP) is required for the development of vascular as well as hematopoietic system in embryoid bodies. *Genes Cells* 2006; **11**: 719–29.
10 Alliegro MC, Alliegro MA. A nuclear protein regulated during the transition from active to quiescent phenotype in cultured endothelial cells. *Dev Biol* 1996; **174**: 288–97.
11 Alliegro MC, Alliegro MA. Identification of a new coiled body component. *Exp Cell Res* 1996; **227**: 386–90.
12 Alliegro MC, Alliegro MA. Protein heterogeneity in the coiled body compartment. *Exp Cell Res* 1998; **239**: 60–8.
13 Ogg SC, Lamond AI. Cajal bodies and coilin–moving towards function. *J Cell Biol* 2002; **159**: 17–21.
14 Blank M, Weinschenk T, Priemer M, Schluesener H. Systematic evolution of a DNA aptamer binding to rat brain tumor microvessels. selective targeting of endothelial regulatory protein pigpen. *J Biol Chem* 2001; **276**: 16464–8.
15 Alliegro MC, Alliegro MA. Nuclear injection of anti-pigpen antibodies inhibits endothelial cell division. *J Biol Chem* 2002; **277**: 19037–41.
16 Alliegro MC. Pigpen and endothelial cell differentiation. *Cell Biol Int* 2001; **25**: 577–84.


© 2010 Japanese Cancer Association

**Molecular Pharmacology Fast Forward. Published on January 22, 2010 as doi:10.1124/mol.109.061481**

MOL#61481

**Title page**

# Sphingosine 1-Phosphate Regulates Vascular Contraction via $S1P_3$ Receptor: Investigation Based on a New $S1P_3$ Receptor Antagonist

Akira Murakami, Hiroshi Takasugi, Shinya Ohnuma, Yuuki Koide, Atsuko Sakurai, Satoshi Takeda, Takeshi Hasegawa, Jun Sasamori, Takashi Konno, Kenji Hayashi, Yoshiaki Watanabe, Koji Mori, Yoshimichi Sato, Atsuo Takahashi, Naoki Mochizuki, and Nobuyuki Takakura

Tokyo Research Laboratories, Drug Research Department, TOA EIYO Ltd., Saitama, Japan (A.M., H.T., S.O., Y.K., Y.S.); Fukushima Research Laboratories, Drug Research Department, TOA EIYO Ltd., Fukushima, Japan (T.H., J.S., T.K., K.H., Y.W., K.M., A.T.); Department of Emergency Medicine, Jikei University School of Medicine, Tokyo, Japan (S.T.); Department of Structural Analysis, National Cardiovascular Center Research Institute, Osaka, Japan (A.S., N.M.); and Department of Signal Transduction, Research Institute for Microbial Diseases, Osaka University, Osaka, Japan (N.T.)



**Copyright 2010 by the American Society for Pharmacology and Experimental Therapeutics.**

**Running title page**

a) Vascular Contraction Regulated by $S1P_3$ Receptor

b) Address correspondence to:

Name; Akira Murakami

Address; Drug Research Department, Tokyo Research Laboratories, TOA EIYO Ltd., 2-293-3 Amanuma, Omiya, Saitama 330-0834, Japan.

Telephone; +81-48-647-7971 Fax; +81-48-648-0078

E-mail; murakami.akira@toaeiyo.co.jp

c) 40 pages of text, 0 tables, 9 figures, 39 references

Abstract; 220 words, Introduction; 547 words, Discussion; 1152 words

d) Abbreviations:

S1P, sphingosine 1-phosphate; GPCR, G protein-coupled receptor; TY-52156, 1-(4-chlorophenylhydrazono)-1-(4-chlorophenylamino)-3,3-dimethyl-2-butanone; MAPK, mitogen-activated protein kinase; CF, coronary flow; CHO-K1, Chinese hamster ovary; HUVECs, human umbilical vein endothelial cells; HCASMCs, human coronary artery smooth muscle cells; Fura-2 AM, Fura-2 pentaacetoxymethylester; SBP, systemic blood pressure; HR, heart rate; MBP, mean blood pressure

**Abstract**

Sphingosine 1-phosphate (S1P) induces diverse biological responses in various tissues by activating specific G protein-coupled receptors ($S1P_1$-$S1P_5$ receptors). The biological signaling regulated by $S1P_3$ receptor has not been fully elucidated because of the lack of a $S1P_3$ receptor-specific antagonist or agonist. We developed a novel $S1P_3$ receptor antagonist, 1-(4-chlorophenylhydrazono)-1-(4-chlorophenylamino)-3,3-dimethyl-2-butanone (TY-52156), and show here that the S1P-induced decrease in coronary flow (CF) is mediated by $S1P_3$ receptor. In functional studies, TY-52156 showed sub-micromolar potency and a high degree of selectivity for $S1P_3$ receptor. TY-52156, but not an $S1P_1$ receptor antagonist (VPC23019) or $S1P_2$ receptor antagonist (JTE013), inhibited the decrease in CF induced by S1P in isolated perfused rat hearts. We further investigated the effect of TY-52156 on both the S1P-induced increase in intracellular calcium ($[Ca^{2+}]_i$) and Rho activation that are responsible for the contraction of human coronary artery smooth muscle cells. TY-52156 inhibited both the S1P-induced increase in $[Ca^{2+}]_i$ and Rho activation. In contrast, VPC23019 and JTE013 inhibited only the increase in $[Ca^{2+}]_i$ and Rho activation, respectively. We further confirmed that TY-52156 inhibited FTY-720-induced $S1P_3$ receptor-mediated bradycardia in vivo. These results clearly show that TY-52156 is both sensitive and useful as a $S1P_3$ receptor-specific antagonist, and reveal that S1P induces vasoconstriction by directly activating $S1P_3$ receptor and through a subsequent increase in $[Ca^{2+}]_i$ and Rho activation in vascular smooth muscle cells.

**Introduction**

Sphingosine 1-phosphate (S1P) is a bioactive lysophospholipid mediator that is mainly released from activated platelets and induces many biological responses, including angiogenesis, vascular development and cardiovascular function (Siess, 2002; Takuwa et al., 2008; Yatomi, 2006). A wide variety of biological cellular responses to S1P have been ascribed to the presence of five S1P receptors, $S1P_1$-$S1P_5$ receptors, that belong to the family of G protein-coupled receptors (GPCRs). Furthermore, a variation of heterotrimeric G protein downstream of S1P receptors accounts for the diversity of cellular responses to S1P (Rosen et al., 2009). In addition to the coupling of S1P receptors and G proteins, the expression of the combination of S1P receptors determines multiple cellular responses. To identify the signaling that is specific for each receptor, S1P receptor antagonists have been developed and have contributed to our understanding of S1P-mediated signaling (Huwiler and Pfeilschifter, 2008).

$S1P_1$-$S1P_5$ receptors couple to different G proteins upon binding to S1P. While, $S1P_1$, $S1P_4$ and $S1P_5$ receptors mainly couple to Gi, $S1P_2$ and $S1P_3$ receptors couple to Gi, Gq and $G_{12/13}$ (Rosen et al., 2009). The signal that converges from Gi-coupled S1P receptors inhibits the activation of adenylate cyclase and induces the activation of p44/p42 mitogen-activated protein kinase (MAPK). While $S1P_1$ receptor slightly increases intracellular calcium ($[Ca^{2+}]_i$) through Gβγ, $S1P_2$ and $S1P_3$ receptors mainly increase $[Ca^{2+}]_i$ through the activation of phospholipase C (PLCβ) from Gq (Watterson et al., 2005). The deletion of $S1P_3$, but not $S1P_2$ receptor in mouse embryonic fibroblasts (MEFs) led to the marked inhibition of S1P-induced PLC activation, which suggests that $S1P_3$ receptor plays an important role in the S1P-induced increase in $[Ca^{2+}]_i$ (Ishii et al., 2002).

$S1P_2$ and $S1P_3$ receptors also couple to $G_{12/13}$ protein to activate a small GTPase, Rho, which is involved in the regulation of actin-cytoskeleton (Ryu et al., 2002; Sugimoto et al., 2003). Rho kinase is activated by Rho through the $G_{12/13}$-Rho guanine nucleotide exchange factor family. S1P-induced Rho activation has been shown to be significantly reduced in $S1P_2$, but not $S1P_3$, receptor-null MEFs (Ishii et al., 2002). Meanwhile, an association between $S1P_3$ receptor and Rho activation has been reported in cells expressing $S1P_3$ receptor (Sugimoto et al., 2003). An S1P-induced contraction of vascular smooth muscle cells has been ascribed to an increase in $[Ca^{2+}]_i$ and Rho activation (Ohmori et al., 2003; Watterson et al., 2005). S1P-induced vasoconstriction is significantly inhibited in cerebral arteries isolated from $S1P_3$ receptor-null mice, but not in those from $S1P_2$ receptor-null mice (Salomone et al., 2008). In addition, Y-27632, a selective Rho kinase inhibitor, inhibits S1P-induced vasoconstriction in canine cerebral arteries (Tosaka et al., 2001), indicating that $S1P_3$ receptor plays an indispensable role in S1P-induced vasoconstriction mediated by Rho-Rho kinase signaling. Although S1P decreases coronary flow (CF) in isolated perfused canine heart, the receptor subtype that is responsible for the S1P-induced reduction of CF has not yet been fully identified. To distinguish $S1P_3$ receptor-dependent signal from $S1P_2$ receptor-dependent signal, a $S1P_3$ receptor-specific antagonist has been needed.

We have developed an $S1P_3$ receptor antagonist, 1-(4-chlorophenylhydrazono)-1-(4-chlorophenylamino)-3,3-dimethyl-2-butanone (TY-52156). By confirming that TY-52156 has a selective antagonistic effect toward $S1P_3$ receptor, we can delineate the role of $S1P_3$ receptor-specific signaling in vascular contraction. Moreover, the effectiveness of TY-52156 in vivo was bolstered by evidence that $S1P_3$ receptor-dependent bradycardia was suppressed by the oral

administration of TY-52156.

## Materials and Methods

### Materials

TY-52156 was synthesized in our laboratories. Materials were purchased from the following suppliers: S1P from BIOMOL International, L.P. (Plymouth Meeting, PA, USA); SEW2871, FTY-720 and FTY-720 (*S*)-Phosphate from Cayman Chemical (Ann Arbor, MI, USA); VPC23019 from Avanti Polar Lipids, Inc. (Alabaster, AL, USA); JTE013 from Tocris Bioscience (Southampton, UK); U46619 from Calbiochem (Darmstadt, Germany); HuMedia-EG2 and HuMedia-SG2 from Kurabo (Osaka, Japan); and membranes containing human $S1P_1$, $S1P_2$, $S1P_3$, or $S1P_5$ receptors from Millipore (Bedford, MA, USA).

### Synthesis of TY-52156

5,5-Dimethyl-2,4-dihexanone (**1**)

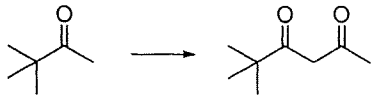

Diisopropyl ether (3 L) was placed in a 5 L 3-neck round-bottom flask and stirred mechanically. Potassium *tert*-butoxide (324 g, 2.25 mol, 1.5 eq) was suspended in the diisopropyl ether at 0 °C. Pinacolone (150 g, 1.50 mol, 1.0 eq) in ethyl acetate (440 mL, 4.50 mol, 3.0 eq) was slowly added dropwise so that the temperature would remain below 10 °C under ice-bath cooling. The reaction mixture was then stirred for 20 h at ambient temperature. Water (1 L) was added slowly so that the temperature would remain below 10 °C under ice-bath cooling. The separated organic layer was extracted with 1N sodium hydroxide (150 mL). The basic aqueous layer was carefully acidified with 6 N HCl (750 mL, 2.0 equivalents of base) at 0 °C and then extracted twice with

petroleum ether (750 mL). The combined organic layer was washed with water (475 mL) and saturated brine (475 mL), dried over anhydrous sodium sulfate, filtered and evaporated at 200 mm Hg and ambient temperature. The remaining liquid was distilled under reduced pressure, with heating up to 80 °C. The title compound (**1**) was obtained as a colorless oil (126 g, 0.89 mol, 59%); $^1$H-NMR (300 MHz, $CDCl_3$) δ: 1.17 (s, 9 H), 2.08 (s, 3 H), 5.61 (s, 1 H); bp.: 62-69 °C (20 mmHg).

3-Chloro-5,5-dimethyl-2,4-dihexanone (**2**)


5,5-Dimethyl-2,4-dihexanone (**1**) (35.4 g, 249 mmol, 1.0 eq) was dissolved in chloroform (700 mL) and stirred mechanically. Sulfuryl chloride (260 mL, 324 mmol, 1.3 eq) in chloroform (130 mL) was slowly added dropwise so that the temperature would remain below 5 °C under ice-bath cooling. The reaction mixture was then stirred for 2 h at 25 °C, and then quenched with water (500 mL) at 0 °C. The separated organic layer was washed three times with water (500 mL), dried over anhydrous sodium sulfate, filtered and evaporated. The residue was purified by distillation under reduced pressure, with heating to 70 °C. The title compound (**2**) was obtained as a yellow oil (41.5 g, 235 mmol, 94%); $^1$H-NMR (300 MHz, $CDCl_3$) δ: 1.23 (s, 9 H), 2.38 (s, 3 H), 5.09 (s, 1 H); bp.: 67-69 °C (1.5 mmHg).

[1-Chloro-1-(4-chlorophenylhydrazono)]-3,3-dimethyl-2-butanone (**3**)

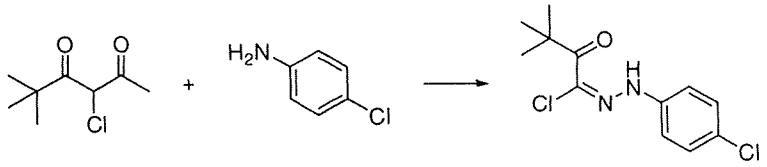

4-Chloroaniline (29 g, 226 mmol, 1.0 eq) was added to 6 N hydrochloric acid (158 mL, 951 mmol, 4.2 eq) and water (68 mL) and stirred for 15 min at 0 °C. Sodium nitrite (17 g, 249 mmol, 1.1 eq) in water (90 mL) was slowly added dropwise so that the temperature would remain below 5 °C under ice-bath cooling. The reaction mixture was stirred for 1 h at 0 °C to prepare a solution of diazonium salt. 3-Chloro-5,5-dimethyl-2,4-dihexanone (**2**) (40 g, 226 mmol, 1.0 eq) was dissolved in pyridine (158 ml) and water (158 mL) at 0 °C. The previously prepared diazonium salt solution was slowly added dropwise so that the temperature would remain below 10 °C, and the resulting mixture was then vigorously stirred for 2 h, with warming from 0 to 25 °C. The reaction mixture was extracted with ethyl acetate (452 mL), washed twice with 2N HCl (1 L) and saturated brine (452 mL), dried over anhydrous sodium sulfate, filtered and evaporated. The resulting crude product was diluted with methanol (226 ml, 1M solution), refluxed for 1 h and then cooled to 0 °C. The precipitated crude crystals were collected by filtration, washed with petroleum ether, and dried under reduced pressure to give the title compound (**3**) as a yellow solid (24 g, 89 mmol, 39%); $^1$H-NMR (300 MHz, $CDCl_3$) δ: 1.43 (s, 9H), 7.12 (d, $J$ = 8.7 Hz, 2H), 7.33 (d, $J$ = 8.7 Hz, 2H), 8.34 (s, 1H); m.p.: 129-131 °C.

2-(4-Chlorophenylhydrazono)-2-(4-chlorophenylamino)acetophenone (**TY-52156**)

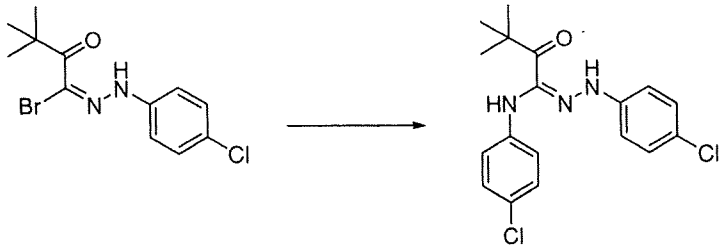

[1-Chloro-1-(4-chlorophenylhydrazono)]-3,3-dimethyl-2-butanone (**3**) (22.4 g, 82.1 mmol, 1.0 eq) and 4-chloroaniline (11.5 g, 90.4 mmol, 1.1 eq) were dissolved in ethanol (274 mL), and triethylamine (13.7 mL, 98.6 mmol, 1.2 eq) was then added at 0 °C. The resulting mixture was stirred for 3 h at ambient temperature. The reaction mixture was evaporated, quenched with water (82 mL), and diluted with ethyl acetate (165 mL). The organic layer was washed with water (165 mL) and saturated brine (165 mL), dried over anhydrous sodium sulfate, filtered and evaporated. The resulting crude crystals were washed with a solvent mixture of hexane-ethyl acetate (20:1) and dried under reduced pressure to obtain the title compound (**TY-52156**) as a yellow powder (24.8 g, 68.1 mmol, 83%); $^1$H-NMR (300 MHz, $CDCl_3$) δ: 1.48 (s, 9H), 6.55 (d, $J$ = 8.4 Hz, 2H), 6.76 (s, 1H), 6.98 (d, $J$ = 8.8 Hz, 2H), 7.19-7.26 (m, 5H); MS (ESI) m/z = 362 $(M-H)^-$; mp.: 90-91 °C.

**Cell Culture**

Chinese hamster ovary (CHO-K1) cells that stably expressed human $S1P_1$ ($S1P_1$-CHO), $S1P_2$ ($S1P_2$-CHO) or $S1P_3$ ($S1P_3$-CHO) receptors were maintained as described previously (Koide et al., 2007). A human recombinant $S1P_4$ receptor-expressing cell line ($S1P_4$-Chem) was purchased from Millipore. Human umbilical vein endothelial cells (HUVECs) purchased from DS Pharma Biomedical (Osaka, Japan) were cultured on collagen-coated dishes in HuMedia-EG2. Human coronary artery smooth muscle

cells (HCASMCs) purchased from Kurabo were cultured in HuMedia-SG2.

**Measurement of the Intracellular Calcium Concentration**

$[Ca^{2+}]_i$ in $S1P_1$-, $S1P_2$-, $S1P_3$-CHO, and $S1P_4$-Chem was measured using the calcium-sensitive dye Fura-2 AM, as described previously (Koide et al., 2007). The fluorescence (excitation at 340 and 380 nm; emission at 510 nm) was measured with a FLEXStation II (Molecular Devises). The ratio of the fluorescence intensity at two wavelengths (FR340/380) was calculated. The *K*i value for TY-52156 was estimated from $Ca^{2+}$ responses as described previously (Ohta et al., 2003).

**[$^3$H]-S1P Binding Assay**

A [$^3$H]-S1P binding assay was performed as described by Lim et al. (2003) with minor modifications. The cell membrane (60 μg/mL) was incubated with binding buffer containing [$^3$H]-S1P (1 nM, about 40,000 dpm per well) and vehicle or each concentration of TY-52156 (μM) for 30 min at 25°C. Radioactivity was measured by a liquid scintillation counter after the addition of scintillation cocktail solution. Nonspecific binding was defined as the amount of radioactivity bound to the cells in the presence of unlabeled S1P (3.0 μM). Specific binding was calculated by subtracting nonspecific binding from total binding.

**GTP-binding Assay**

Europium-GTP (Eu-GTP) binding was determined using a DELFIA GTP Binding Assay Kit (Perkin-Elmer Life Sciences, Wallac, Turku, Finland). Samples were incubated in AcroWell filter plates (PALL, Ann Arbor, MI, USA) for 60 min ($S1P_1$ and $S1P_5$) or 90

min ($S1P_2$ and $S1P_3$) at 30°C. The reaction was started by adding membranes (48 μg/mL) containing human $S1P_1$, $S1P_2$, $S1P_3$ or $S1P_5$ receptors to the assay buffer (20 mM HEPES, pH7.4, 5 mM $MgCl_2$, 100 mM NaCl, 1.2 mg/mL Saponin, 10 μM GDP and 10 nM Eu-GTP at 30°C) including S1P (0.1 μM) and vehicle or the desired concentration (μM) of the test drug (TY-52156 or VPC23019). The reaction was terminated by rapid filtration and the filter was washed five times with 200 μL of ice-cold washing solution in a vacuum manifold. The plate was measured by time-resolved fluorescence (340 nm excitation/615 nm emission) using a EnVision (Perkin-Elmer Life Sciences).

**Western Blot Analysis for p44/p42 MAPK**

$S1P_1$-, $S1P_2$- and $S1P_3$-CHO ($2.0\times10^5$ cells) were plated on 6-well plates and cultured with Nutrient Mixture F-12 Ham (Sigma) containing 1% FBS for 4 h before the experiments. The cells were treated with vehicle, TY-52156 (TY) (10 μM), VPC23019 (VPC) (10 μM) or JTE013 (JTE) (1.0 μM) for 10 min and then with vehicle or S1P (0.1 μM) for 5 min at 37°C. The cells were lysed in CelLyticM containing Protease Inhibitor Cocktails and Phosphatase Inhibitor Cocktails (Sigma) for 10 min at 4°C. The lysate was centrifuged at 13,000×g for 15 min at 4°C and supernatant was transferred to a fresh tube. The protein concentration was determined using the Bradford method. Equal amounts of proteins were resuspended in 4×Sample Buffer (Wako Pure Chemical Industries), boiled for 5 min and separated by 10% SDS-PAGE. After being transferred to a polyvinylidene fluoride (PVDF) membrane, the membranes were blocked in Block Ace (DS Pharma Biomedical) and immunoblotted with antibodies of phospho-p44/p42 MAPK or p44/p42 MAPK (1:1000, Cell Signaling

Technology). The signals were visualized by an Amplified Alkaline Phosphatase Goat Anti-Rabbit Immun-Blot Assay Kit (Bio-Rad) according to the manufacturer's instructions. Quantitative analyses of immunoblots were performed using Quantity One version 4.2.2 software (Bio-Rad). The relative percentage compared with the vehicle was calculated and expressed as the mean±S.E.M.

**Measurement of Coronary Flow**

All animal experiments were reviewed and approved by the Experimental Animal Committee in our laboratories. Male Sprague–Dawley (SD) rats (300-350 g; Nihon SLC) were anesthetized by the injection of pentobarbital (50 mg/kg i.p.). After thoracotomy, their hearts were rapidly excised and perfused at 37°C in a Langendorff manner with Krebs-Henseleit bicarbonate buffer (constant perfusion pressure of 70±5 mmHg) of the following composition (in mM): NaCl 118; KCl 4.7; $KH_2PO_4$ 1.2; $MgSO_4$ 1.2; $CaCl_2$ 2.5; $NaHCO_3$ 24.9; EDTA/2Na 0.027; ascorbic acid 0.057 and glucose 11.1, pH 7.4 at 37°C, bubbled with 95% $O_2$ and 5% $CO_2$ ($pO_2$>550 mmHg). A modified water-filled latex balloon (LB-2, Technical Service Corporation) was inserted into the left ventricle via the left atrium with a pressure transducer (DX-360, Ohmeda) connected to an amplifier (AP-601G, Nihon Kohden). Left ventricular end-diastolic pressure was adjusted to about 5-10 mmHg. To measure coronary flow (CF), a Cannulating-type Flow Probe (FF-030T, Nihon Kohden) connected to an electro-magnetic blood-flow meter (MFV-3700, Nihon Kohden) was inserted to the perfusion line that was connected to the heart. After a 15-min period for equilibration, vehicle, TY-52156 (TY) (0.1 μM), VPC23019 (VPC) (0.1 μM) or JTE013 (JTE) (0.1 μM) was infused for 10 min by an infusion pump (Harvard Apparatus) through a

drug-infusion line connected to the main perfusion line at a flow rate of 1/100 the CF rate. After drug treatment, vehicle or the indicated concentration of S1P (μM) or U46619 (0.1 μM) was added to the same line. CF was measured before and 10 min after the infusion of S1P or U46619. The relative percentage compared to the vehicle was calculated from the CF rate.

**Contractile Response in Cerebral Arteries**

Beagle dogs (Oriental Yeast) were anesthetized by the injection of pentobarbital (30 mg/kg i.p.). The cerebral arteries were rapidly excised and mounted in organ chambers containing Krebs buffer of the following composition (in mM): NaCl 118.0, KCl 4.7, $CaCl_2$ 2.5, $KH_2PO_4$ 1.2, $MgSO_4$ 1.2, $NaHCO_3$ 25.0 and glucose 11.0, pH 7.2 at 37°C, bubbled with 95% $O_2$ and 5% $CO_2$. After equilibration, cerebral arteries were exposed to 60 mM KCl until the contractile responses were stabilized. After washout and recovery, contractile responses to S1P were measured every 10 min after the addition of the indicated concentration of S1P (μM). In another experiment, the cerebral arteries were contracted by S1P (5.0 μM), and then an increasing amount of vehicle or TY-52156 (up to 10 μM) was applied to the organ chambers. Relaxation responses were measured every 10 min after addition of the indicated concentration of vehicle or TY-52156 (μM). The degree of contraction compared to vehicle was calculated with PRISM version 4 statistical software (GraphPad) and expressed as the percent contraction compared to that induced by S1P.

**Immunoprecipitation and Western Blot**

HCASMCs were seeded at $5\times10^5$ cells in a culture dish. After they reached

confluence, cells were pretreated with vehicle or the indicated concentration (μM) of test drug for 10 min, and then with vehicle or S1P (0.1 μM) for 3 min at 37°C. The amounts of activated Rho (GTP-Rho) were measured by a Rho Activation Assay Biochem Kit (Cytoskeleton) according to the manufacturer's instructions. Quantitative analysis was performed as described above. The density ratio of GTP-Rho to total Rho was measured and its vehicle value was set to 1.0.

**Pharmacokinetic Analysis**

Male SD rats were purchased from Nihon SLC. Blood samples were collected from the jugular vein at 1, 2, 4, 6, 8 and 24 h after the start of the administration of TY-52156-HCl. Samples were placed into sodium heparinized tubes and subjected to centrifugation at 14,000×g for 10 min at 4°C to separate the plasma. Plasma concentrations were quantified by an API 4000 (TM) LC/MS/MS System (Applied Biosystems/MDS SCIEX, Ontario, Canada). The mean peak plasma concentration ($C_{max}$) and time to reach $C_{max}$ ($T_{max}$) were estimated from actual measurements. The half-life ($T_{1/2}$) was calculated with WinNonlin ver. 2.1 software (Pharsight, Mountain View, CA).

**Measurement of Systemic Blood Pressure, Heart Rate and Mean Blood Pressure**

Male SD rats (290-340 g) were purchased from Nihon SLC. Systemic blood pressure (SBP) and heart rate (HR) were measured in the conscious state with a tail-cuff blood pressure analyzer (MK2000, Muromachi-kikai). In another experiment, SD rats were anesthetized by the injection of pentobarbital (50 mg/kg i.p.) and cannulas were placed in a carotid artery and femoral vein. Mean blood pressure (MBP) was measured with a

pressure transducer (DX-360) that was connected to the cannula placed in a carotid artery. HR was measured with a tachometer (1321; NEC-San-ei). MBP and HR were measured before, and 10 and 20 min after the injection of FTY-720 (1.0 mg/kg i.v.).

**Statistical Analysis**

Experimental values are expressed as mean±S.E.M. The Student *t*-test or ANOVA followed by Dunnett's multiple-comparison test was used to statistically analyze differences between groups. $P< 0.05$ was considered to be significant.